Can SUSY relax lepton number violation constraints coming from loop corrections to light neutrino masses on the low-scale seesaw mechanism?

J. Jones-Pérez * and O. Suarez-Navarro †

Sección Física, Departamento de Ciencias, Pontificia Universidad Católica del Perú, Apartado 1761, Lima, Peru

(Received 24 February 2023; accepted 17 May 2023; published 1 June 2023)

Heavy neutrinos from the type-I seesaw model can have a large mixing with active states, motivating their search at collider experiments. However, loop corrections to light neutrino masses constrain the heavy neutrinos to appear in pseudo-Dirac pairs, leading to a potential suppression of lepton number violating parameters. In this work we perform a detailed review of a proposal to relax constraints on lepton number violation by adding supersymmetry (SUSY). We define the conditions necessary to maximize the SUSY screening effect, with the objective of allowing a larger mass splitting between low-scale heavy neutrino masses. We find that the sole addition of SUSY does not guarantee a screening, and that favorable cases have some degree of fine-tuning.

DOI: 10.1103/PhysRevD.107.115003

I. INTRODUCTION

The type-I seesaw [1–5] is very likely the most studied extension of the Standard Model (SM) explaining neutrino masses. One of its key predictions is the existence of heavy neutrinos N_h, although their number, mass scale, and coupling strength remain free parameters. This has motivated their search by several experiments (see reviews [6–8]) with unfortunately null signals to date.

It is well known that, in its most basic realization, the seesaw is actually very hard to test. The N_h interact via their mixing with the active flavor states (ν_e, ν_μ, ν_τ), and the typical expectation is that the square of this mixing will be proportional to the ratio between light and heavy neutrino masses, out of reach of current and near future experiments. This theoretical constraint can be evaded once the model includes at least two heavy neutrinos, introducing textures in the neutrino mass matrix that reproduce light neutrino masses and permit the mixing to be significantly enhanced [9]. Thus, the aforementioned searches for N_h, which generally interpret their results in terms of one heavy neutrino with large mixing, could be considered as probing seesaw scenarios with several heavy neutrinos, but with only one of them having a mass within the reach of the experiment.

Unfortunately, this view is not acceptable. When heavy neutrinos have enhanced mixing and large splitting between their masses, the mass matrix has strong cancellations between its elements, induces large contributions to neutrinoless double beta decay ($0\nu\beta\beta$), and leads to unacceptable quantum corrections to light neutrino masses [10–17]. Even though the cancellations in the mass matrix can be justified by the presence of a lepton number (LN) symmetry, whose breaking generates the light neutrino masses [18–21], the constraints by $0\nu\beta\beta$ and loop corrections can only be avoided if, in addition, the heavy neutrinos appear in almost degenerate pairs at tree level, usually called pseudo-Dirac neutrinos. The reason for this is that the mass splitting is connected to new sources of lepton number violation (LNV), which at tree level do not participate in the generation of light neutrino masses. Thus, the bounds on the mass splittings suggest that searches for single N_h would not be theoretically well motivated, at least from the seesaw perspective.

An important effect of having pseudo-Dirac heavy neutrinos is that all LNV effects could be heavily suppressed, particularly for large N_h masses. This brings the need of phenomenological reinterpretations of collider searches [22–25], which generally give rise to modifications of the reported bounds.

It must be noted that the bounds coming from loop corrections are theoretical. In principle, it is possible to fine-tune the light neutrino tree-level masses, such that the physical masses are correctly reproduced. Thus, these constraint are based on the desire to avoid fine-tuning between the tree and loop level contributions to physical masses. In this sense, an intriguing option was presented in [26], in the context of a supersymmetric extension of the

*jones.j@pucp.edu.pe
†osuarez@pucp.edu.pe

type-I seesaw. Here, light neutrino masses were generated radiatively, with contributions from both heavy neutrinos and sneutrinos. An interesting conclusion was that large LNV parameters are still allowed in the model, as the new sneutrino loops can help to keep the corrections under control. The origin of this "supersymmetry (SUSY) screening" effect allegedly stems from remnants of the SUSY nonrenormalization theorems [27,28].

This result has interesting implications in our discussion on searches for single heavy neutrinos, regardless of having radiative light neutrino masses or not. If sizeable LNV is permitted, then it would be possible to relax the constraints on N_h mass splittings,[1] allowing a straightforward interpretation of experimental results. Furthermore, the discovery of a single N_h could also be interpreted as a hint in favor of supersymmetry. Thus, we consider it important to further examine the findings of [26] in our context. In addition, we consider that a more detailed explanation of the screening effect is necessary, understanding which SUSY contribution allows for cancellations, and under which circumstances this happens.

In this work we take the supersymmetric extension of the type-I seesaw and explore in depth the possibility of having destructive interference between the SUSY and non-SUSY loop corrections to light neutrino masses, with the intention of allowing large heavy neutrino mixing with large mass splitting. We begin by reviewing the problem of quantum corrections in Sec. II. Then, in Sec. III, we present the ν_RMSSM and calculate the SUSY and non-SUSY loop contributions. Section IV is the most important part of this work, where we evaluate when is it feasible to have cancellations between SUSY and non-SUSY loops. We conclude in Sec. V where, given our findings, we argue that due to the experimental constraints on SUSY masses the screening is not a generic feature of supersymmetry and actually happens in very specific scenarios.

II. LOOP CORRECTIONS IN THE STANDARD SEESAW

The type-I seesaw models generate light neutrino masses via the introduction of N new heavy neutral leptons ν_R. These are also called sterile neutrinos, in contrast to the active neutrinos within $SU(2)_L$ doublets. In the model, the full neutrino mass matrix on the active-sterile basis is

$$M_\nu^{\text{tree}} = \begin{pmatrix} 0 & M_D \\ M_D^T & M_R \end{pmatrix}. \tag{1}$$

For "large" M_R one can obtain the light neutrino masses to an excellent approximation by diagonalizing the matrix:

$$M_{\text{light}}^{\text{tree}} = -M_D M_R^{-1} M_D^T. \tag{2}$$

On the standard seesaw model, the heavy neutrinos couple to Standard Model particles via the mixing matrix U, which diagonalizes the full mass matrix shown in Eq. (1). When including $N = 3$ sterile neutrinos, this matrix can be decomposed into four 3×3 blocks:

$$U = \begin{pmatrix} U_{a\ell} & U_{ah} \\ U_{s\ell} & U_{sh} \end{pmatrix}. \tag{3}$$

Throughout this paper, a indices denote the active basis where the charged lepton Yukawas Y_e are diagonal, i.e., $a = e, \mu, \tau$. The $s = s_1, s_2, s_3$ indices denote the sterile neutrino basis, which at this point is arbitrary. In addition, $\ell = 1, 2, 3$ labels the three light (mostly active) neutrinos n_ℓ, with masses m_1, m_2, m_3, while $h = 4, 5, 6$ labels the three heavier (mostly sterile) neutrinos N_h, with masses M_4, M_5, M_6.

For our numerical results, we shall take a specific choice of parameters such that, in the case of normal ordering of light neutrino masses, we can write the U_{ah} mixing as [14,29–31]

$$U_{a4} = i(U_{\text{PMNS}})_{a1}\sqrt{\frac{m_1}{M_4}}, \tag{4}$$

$$U_{a5} = z_{56} Z_a \sqrt{\frac{m_3}{M_5}} \cosh\gamma_{56} e^{iz_{56}\rho_{56}}, \tag{5}$$

$$U_{a6} = i Z_a \sqrt{\frac{m_3}{M_6}} \cosh\gamma_{56} e^{iz_{56}\rho_{56}}, \tag{6}$$

$$Z_a = (U_{\text{PMNS}})_{a3} + i z_{56}\sqrt{\frac{m_2}{m_3}}(U_{\text{PMNS}})_{a2}, \tag{7}$$

where z_{56} is the sign of the free parameter $\gamma_{56} \gtrsim 2$, and $\rho_{56} \in [0, \pi/2]$. From here it is possible to reconstruct the Dirac and Majorana masses appearing in Eq. (1). If we take $\hat{M}_h = \text{diag}(M_4, M_5, M_6)$, we can write $M_D = U_{ah}^* \hat{M}_h$ and $M_R = \hat{M}_h$.

We see that both U_{a5} and U_{a6} can be enhanced, in this case by a factor $\cosh\gamma_{56}$, while U_{a4} remains small. Thus, by taking a very large M_4 we can decouple this heavy neutrino, leaving us with an effective $3 + 2$ seesaw model. As mentioned in the Introduction, this possibility of enhancing the active-heavy mixing while keeping acceptable light neutrino masses can be attributed to a slightly broken lepton number symmetry [18–21].

Loop corrections can modify both M_D and M_R, as well as generate a nonzero element in the active-active region of M_ν^{tree}, which can be denoted by δM_D, δM_R, and δM_L, respectively. Nevertheless, from these the most important correction to light neutrino masses comes from δM_L, such that one can write

[1]Large mass splittings would still need to be compatible with $0\nu\beta\beta$.

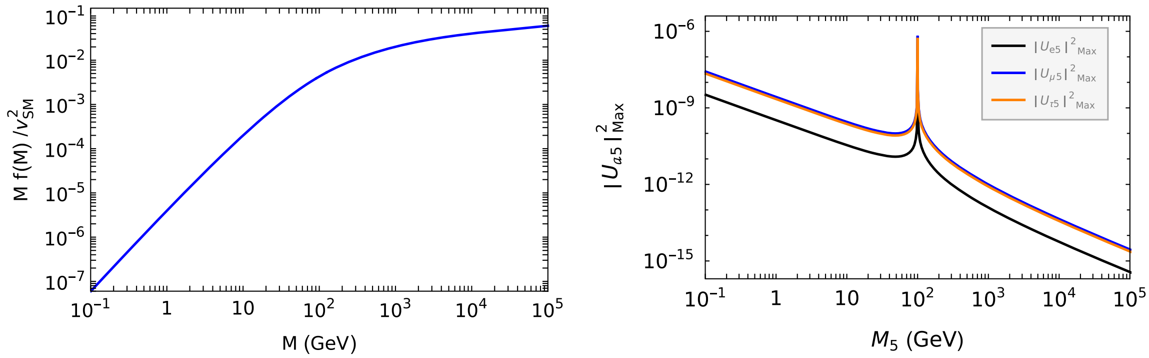

FIG. 1. Left: dependence of loop function, conveniently normalized, with respect to heavy neutrino mass. Right: maximum value of $|U_{a5}|^2$ as a function of M_5, for $M_6 = 100$ GeV.

$$M^{\rm full}_{\rm light} = M^{\rm tree}_{\rm light} + \delta M_L. \tag{8}$$

In this standard seesaw model, δM_L is determined by loops involving the Z and H^0 bosons. Diagrams including the W boson would not contribute at one loop, as there would be no LNV term on any vertex or propagator. The well-known result for δM_L [32–34] can be written in our notation:

$$(\delta M_L)_{aa'} = \frac{1}{v^2_{\rm SM}} \sum_{h,s,s'} (M_D)_{as} U_{sh} (M_D)_{a's'} U_{s'h} f(M_h), \tag{9}$$

$$\approx \frac{m_3}{v^2_{\rm SM}} Z^*_a Z^*_{a'} [M_5 f(M_5) - M_6 f(M_6)] \cosh^2 \gamma_{56} e^{-2iz_{56}\rho_{56}}, \tag{10}$$

where the loop function $f(M_h)$ is defined:

$$f(M_h) = \frac{M_h}{16\pi^2} \left[3 \left(\frac{M_h^2}{M_Z^2} - 1 \right)^{-1} \ln \frac{M_h^2}{M_Z^2} + \left(\frac{M_h^2}{M_H^2} - 1 \right)^{-1} \ln \frac{M_h^2}{M_H^2} \right]. \tag{11}$$

In Eq. (10) we have written the correction in our benchmark scenario, Eqs. (4)–(6), neglecting the contribution of N_4.

The dependence of $f(M_h)$ as a function of the heavy neutrino mass can be seen on the left panel of Fig. 1, where we have multiplied a normalization factor $M_h/v^2_{\rm SM}$. We see the that loop correction increases with mass, with the slope varying around $M_h \sim 100$ GeV. This change is due to the terms multiplying the logarithms in Eq. (11), which for large M_h adds an additional suppression factor.[2]

From Eq. (9) it is possible to confirm that, if a heavy neutrino does not have an almost degenerate pair, then active-heavy mixing cannot exceed a certain value, or else substantial loop corrections are induced. If this bound is not respected, fine-tuning is required to accurately reproduce the observed neutrino masses [15]. Such upper limits for $|U_{a5}|^2$ are shown as a function of M_5 on the right panel of Fig. 1, for $M_6 = 100$ GeV, where we require loop corrections not to exceed 50% of the tree-level value. For example, for M_5 equal to 1 GeV (1 TeV), we need $\gamma_{56} \lesssim 2.94$ ($\lesssim 2.45$), which corresponds to $|U_{\mu 5}|^2 \lesssim 2.7 \times 10^{-9}$ ($|U_{\mu 5}|^2 \lesssim 9.9 \times 10^{-13}$). Note that the apparent stronger bounds on $|U_{e5}|^2$ are really due to the correlations existing between the mixings such that, given some value for $|U_{\mu h}|^2$ or $|U_{\tau h}|^2$, the different Z_a terms make $|U_{eh}|^2$ smaller. From this result, it is clear that a single heavy neutrino with mass $\gtrsim 1$ GeV cannot have its mixing enhanced by too much, so is unlikely to appear at collider searches.[3]

As a final comment, note that in Eq. (10) one can see that, if $M_5 \to M_6$, there exists a cancellation between the N_5 and N_6 contributions. This leads to the peak shown in the right panel of Fig. 1. As commented earlier, this can again be attributed to the slightly broken lepton number symmetry, which guarantees that loop corrections are kept small [13,15,16]. In this interpretation, degenerate N_h masses imply that the only nonzero sources of LNV are those essential for obtaining nonzero light neutrino masses, so no new LNV terms appear at the loop level. The maximum size of allowed nondegeneracy is critically dependent on the value of $|U_{ah}|^2$ and the average mass, as was shown in [16].

III. THE ν_RMSSM MODEL

The simplest SUSY extension of the standard seesaw consists of introducing $\hat{\nu}^c_R$ superfields to the MSSM. Apart from the sterile neutrinos, this also implies the presence of new scalar partners, the R-sneutrinos $\tilde{\nu}^c_R$. The introduction of SUSY leads to modifications in the light neutrino phenomenology, for example, due to RGEs [35–39]. Of course, here we are interested in the new contributions to

[2]Note that, when M_h is much larger than the electroweak scale, one should actually decouple the heavy neutrinos and use effective operators.

[3]This statement is made evident by comparing our limits with experimental bounds shown in [6–8].

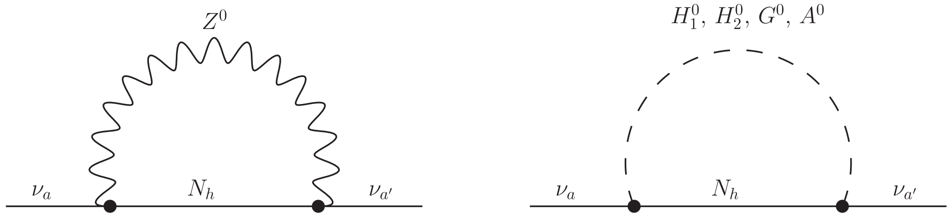

FIG. 2. Nonsupersymmetric one-loop diagrams of the MSSM that contribute to the neutrino mass matrix.

the loop corrections to the neutrino propagator. These can be be either supersymmetric or nonsupersymmetric, the former including loops with neutralinos and sneutrinos, as well as charginos and charged sleptons, and the latter involving the heavier Higgs bosons.

The superpotential of the model is

$$\mathcal{W} = \mathcal{W}_{\mathrm{MSSM}} + (Y_\nu^*)_{as}\hat{L}_a \cdot \hat{H}_u \hat{\nu}^c_{Rs} + \frac{1}{2}(M_R)_{ss'}\hat{\nu}^c_{Rs}\hat{\nu}^c_{Rs'}, \quad (12)$$

where the Yukawas are connected to the Dirac mass via $M_D = \frac{v_{\mathrm{SM}}}{\sqrt{2}} Y_\nu^* \sin\beta$, with $\tan\beta$ being the ratio of the Higgs vacuum expectation values.[4] Note that the parametrization we are using in the neutrino sector determines M_D, from which the Yukawas can be extracted. In addition to the superpotential, the following soft SUSY-breaking terms are allowed:

$$\begin{aligned}\mathcal{V}^{\mathrm{soft}} = \mathcal{V}^{\mathrm{soft}}_{\mathrm{MSSM}} &+ (m^2_{\tilde{\nu}})_{ss'}\tilde{\nu}^c_{Rs}\tilde{\nu}^c_{Rs'} \\ &+ \left(\frac{1}{2}(B_\nu)_{ss'}\tilde{\nu}^c_{Rs}\tilde{\nu}^c_{Rs'} + (T_\nu^*)_{as}\tilde{L}_a \cdot H_u \tilde{\nu}^c_{Rs} + \mathrm{H.c.}\right).\end{aligned} \quad (13)$$

In addition to the typical soft mass $m^2_{\tilde{\nu}}$ and trilinear couplings T_ν, we have a LNV soft mass B_ν. This new term will give further contributions to neutrino masses at the loop level. In fact, B_ν played a major role in [40], in the context of the supersymmetric inverse seesaw with only one pair of sterile neutrinos. Here, they explored the possibility of generating one light neutrino mass via the standard seesaw, and the other through SUSY corrections, with the requirement of having T_ν not aligned with Y_ν.

In the following sections we shall describe both SUSY and non-SUSY loop corrections to the light neutrino masses. Here, and in the following sections, we will focus on heavy neutrino masses discoverable at colliders, namely $M_h = 40$, 200 GeV.

[4]Even though they can be enhanced, the Yukawas are usually very small. For example, following our parametrization in Eqs. (4)–(6), the largest element of $|Y_\nu|$ for a lightest neutrino mass of 10^{-3} eV, heavy neutrino masses of order 100 GeV, and $\gamma_{56} = 8$ is $\sim 5 \times 10^{-4}$.

A. Non-SUSY loop corrections

The full one-loop correction to the neutrino propagator in models with two Higgs doublets has been extensively studied in the past, see for example [32,34,41–45]. The relevant diagrams involve the W and Z bosons, the neutral and charged Higgs bosons, and the corresponding Goldstone bosons. Nevertheless, as in the standard seesaw, loops involving charged particles do not contribute to the Majorana mass, leaving only the diagrams shown in Fig. 2. Although the δM_L correction involving the Z is the same as in the standard seesaw, there is a new combined contribution from the neutral scalars. Thus, in terms of Y_ν, we can write the full correction:

$$(\delta M_L)^{\mathrm{2HDM}}_{aa'} = \frac{1}{2}\sum_{h,s,s'}(Y_\nu^*)_{as}U_{sh}(Y_\nu^*)_{a's'}U_{s'h}g(M_h, M_A, \tan\beta), \quad (14)$$

$$\approx K_{aa'}[M_5 g(M_5, M_A, \tan\beta) - M_6 g(M_6, M_A, \tan\beta)], \quad (15)$$

where the second line again corresponds to our benchmark scenario. We have defined $K_{aa'} = (m_3/v_u^2)Z_a^* Z_{a'}^* \times \cosh^2\gamma_{56} e^{-2iz_{56}\rho_{56}}$, and a new loop function:

$$\begin{aligned} g(M_h, M_A, \tan\beta) = \frac{M_h}{16\pi^2}\Bigg[&3\sin^2\beta\left(\frac{M_h^2}{M_Z^2} - 1\right)^{-1}\ln\frac{M_h^2}{M_Z^2} \\ &+ \cos^2\alpha\left(\frac{M_h^2}{M_{H_1}^2} - 1\right)^{-1}\ln\frac{M_h^2}{M_{H_1}^2} \\ &+ \sin^2\alpha\left(\frac{M_h^2}{M_{H_2}^2} - 1\right)^{-1}\ln\frac{M_h^2}{M_{H_2}^2} \\ &- \cos^2\beta\left(\frac{M_h^2}{M_A^2} - 1\right)^{-1}\ln\frac{M_h^2}{M_A^2}\Bigg]. \end{aligned} \quad (16)$$

Here, M_A, M_{H_1}, and M_{H_2} are the masses of the pseudoscalar and scalar Higgses, and α is the scalar mixing angle. It is important to remember that, at tree level, all of the latter are a function of M_A and $\tan\beta$. In particular, in the decoupling regime, we find a very precise cancellation between the H_2 and A contributions. Notice we do not proceed as in [26], who modify the effective quartic coupling in the scalar mass matrix such that the observed lightest Higgs mass is obtained. The reason is that the

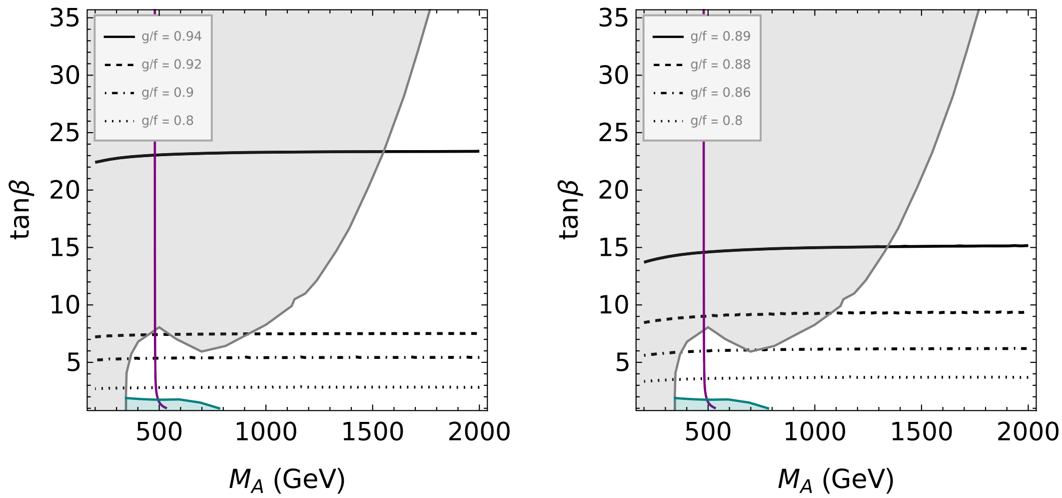

FIG. 3. Ratio between loop functions, $g(M_h, M_A, \tan\beta)/f(M_h)$. Gray (dark green) region is excluded by $H/A \to \tau^+\tau^-$ [46] ($H^\pm \to tb$ [47]) searches. The region to the left of the purple curve is excluded, as here the light Higgs boson couplings do not match with measurements [48]. We show results for $M_h = 40$ (200) GeV on the left (right).

aforementioned cancellation is spoilt, suggesting it might be necessary to include similar corrections in the pseudoscalar mass matrix at the same time, which is outside the scope of this work.

From Eq. (15), we can expect that corrections in general type-II two Higgs doublet models will have a very similar phenomenology to that of the standard seesaw, in particular in what concerns the enhancement to the neutrino mixing and the possibility of cancellations between different heavy neutrino contributions. In our case, the constraints imposed by the SUSY framework appear in the structure of the g function, as shown in Eq. (16), where most of the appearing parameters are related to each other. This leads to g not having a strong dependence on M_A nor $\tan\beta$, with numerical values very similar to the f of the standard seesaw, see Eq. (11). To illustrate this, we shown in Fig. 3 the ratio between g and f, presented as a function of M_A and $\tan\beta$, for two values of M_h. We find that, for the evaluated values of heavy neutrino mass, g is always slightly smaller than f, but hardly decreases under 80%.

Thus, for a given M_D and $\hat{M}_h$, the non-SUSY corrections are expected to be of the same order of magnitude as in the standard seesaw. These will depend on the heavy neutrino masses in a way similar to what is shown on the left panel of Fig. 1. Correspondingly, the larger the $\Delta M_{65} = M_6 - M_5$ mass splitting, the larger the contribution, with its sign being the opposite of that of ΔM_{65}.

B. SUSY loop corrections

As mentioned earlier, SUSY corrections to the light neutrino propagator involve both sneutrino-neutralino and charged slepton-chargino loops. Moreover, since only the $\hat{\nu}_R$ sector involve LNV terms, only the former are relevant for δM_L [26,49,50].

Since we now have two sources of LNV, namely M_R and B_ν, for transparency we will carry out our analysis using the mass-insertion technique [51–55]. This has the additional advantage of being able to carry out our calculations directly on the active-sterile basis. Such an approach was also followed in [26], although here this will be done only for the sneutrino line in the SUSY contribution. For this, we need to write the terms of the sneutrino scalar potential contributing to the sneutrino mass matrix. These can be split into lepton number conserving (LNC) and LNV terms, $\mathcal{L}^{\text{mass}}_{\tilde{\nu}} = \mathcal{L}^{\text{LNC}}_{\tilde{\nu}} + \mathcal{L}^{\text{LNV}}_{\tilde{\nu}}$, where

$$\begin{aligned} -\mathcal{L}^{\text{LNC}}_{\tilde{\nu}} = {} & \tilde{\nu}^*_{La} \underbrace{\left(m^2_{\tilde{L}} + \frac{v_u^2}{2} Y_\nu Y_\nu^\dagger + \frac{1}{2} m_Z^2 \cos 2\beta \right)_{aa'}}_{m^2_{\tilde{\nu}_L}} \tilde{\nu}_{La'} \\ & + \tilde{\nu}^c_{Rs} \underbrace{\left(m^{2T}_{\tilde{\nu}} + \frac{v_u^2}{2} Y_\nu^\dagger Y_\nu + M_R M_R^* \right)_{ss'}}_{m^2_{\tilde{\nu}_R}} \tilde{\nu}^c_{Rs'} \\ & + \tilde{\nu}^c_{Rs} \left(\frac{v_u}{\sqrt{2}} T_\nu^\dagger - \frac{v_d}{\sqrt{2}} \mu^* Y_\nu^\dagger \right)_{sa} \tilde{\nu}_{La} \\ & + \tilde{\nu}^*_{La} \left(\frac{v_u}{\sqrt{2}} T_\nu - \frac{v_d}{\sqrt{2}} \mu Y_\nu \right)_{as} \tilde{\nu}^c_{Rs}, \end{aligned} \tag{17}$$

$$\begin{aligned} -\mathcal{L}^{\text{LNV}}_{\tilde{\nu}} = {} & \tilde{\nu}^c_{Rs} \left(\frac{1}{2} B_\nu \right)_{ss'} \tilde{\nu}^c_{Rs'} + \tilde{\nu}^*_{La} \left(\frac{v_u}{\sqrt{2}} Y_\nu M_R \right)_{as} \tilde{\nu}^c_{Rs} \\ & + \tilde{\nu}_{La} \left(\frac{v_u}{\sqrt{2}} Y_\nu^* M_R^* \right)_{as} \tilde{\nu}^c_{Rs} \end{aligned} \tag{18}$$

Thus, we have LNV mass insertions from Eq. (18), as well as LNC insertions from the last line of Eq. (17). From Eq. (18), we find two types of LNV terms. From these, the $Y_\nu M_R$

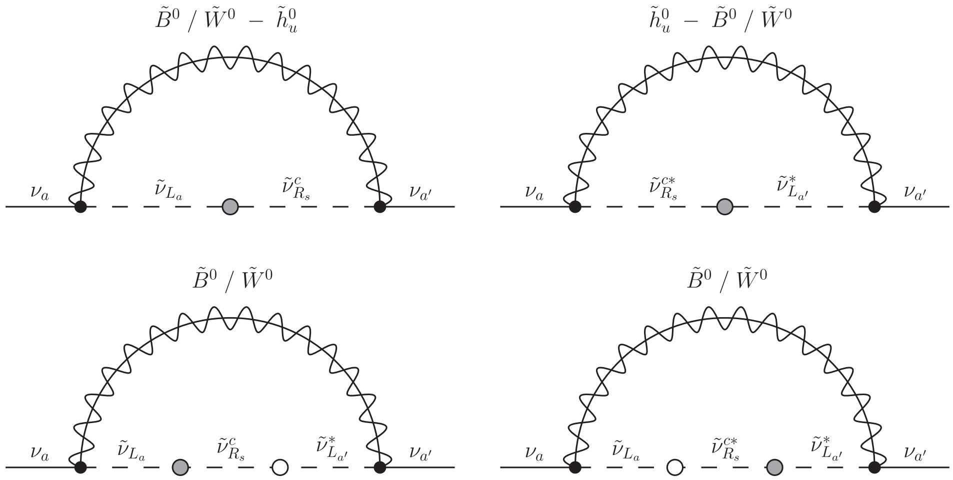

FIG. 4. Irreducible mass insertions. In all cases, gray (white) blobs indicate LNV (LNC) insertions. Top: gaugino-Higgsino case. Bottom: pure gaugino case.

terms are "irreducible" in the sense that they cannot be set to zero without spoiling the seesaw mechanism at tree level. In contrast, a vanishing B_ν does not affect the neutrino masses at leading order, and thus are considered "reducible."

In the following, for simplicity, we assume $m^2_{\tilde{L}}$ and $m^2_{\tilde{\nu}}$ to be diagonal. With this, we can also take the $m^2_{\tilde{\nu}_L}$ and $m^2_{\tilde{\nu}_R}$ matrices as diagonal, to an excellent approximation. In addition, when presenting numerical results, we will take $T_\nu = a_\nu Y_\nu$ and $B_\nu = b_\nu M_R$. Note that these assumptions, which are not guaranteed by SUSY, will be crucial to preserve the flavor structure of the tree-level mass matrix.

In what follows, we list all possible contributions to δM_L up to order $\mathcal{O}(Y^2_\nu)$, which was the assumption taken when writing Eq. (8). For each type of loop diagram, we present both the complete expression and an approximate one relevant for our benchmark scenario, applying our assumptions for T_ν and B_ν, taking degenerate[5] $m_{\tilde{L}}$ and neglecting the contribution from $\tilde{\nu}_{R4}$.

1. Irreducible contributions ($B_\nu = 0$)

Since we are taking terms of order $\mathcal{O}(Y^2_\nu)$, it is crucial to note that the LNV insertions we are currently considering are of the type $(Y_\nu M_R)/M_{\rm SUSY}$, meaning that we will have at most two of these in δM_L. The same reasoning can be followed for the LNC insertions in the last line of Eq. (17). From these considerations, we can expect these SUSY corrections to be negligible if the Yukawas are not enhanced.

Let us consider the pure Higgsino contribution. Here, we have a Y_ν suppression at each vertex, so adding any insertion make these of order larger than $\mathcal{O}(Y^2_\nu)$, and can be neglected.

[5]Exactly degenerate sleptons can induce artificially large mixing. This can be avoided by adding slepton mass splittings at the per-mille level, without spoiling our numerical results.

Next come the gaugino-Higgsino contributions, shown on the top row of Fig. 4, with only one vertex with a Y_ν suppression. We can allow only one mass insertion:

$$
\begin{aligned}
(\delta M_L^{\rm irr})^{gh}_{aa'} &= \frac{v_u}{2}\sum_{b,s,r}(-1)^b g_b \frac{1}{m_{\tilde{\chi}^0_r}} O_{rb} O_{r4} \\
&\quad\times [(Y^*_\nu M^*_R)_{as}(Y^*_\nu)_{a's} f_3(m^2_{\tilde{\chi}^0_r}, m^2_{\tilde{\nu}_{La}}, m^2_{\tilde{\nu}_{Rs}}) \\
&\quad + (Y^*_\nu)_{as}(Y^*_\nu M^*_R)_{a's} f_3(m^2_{\tilde{\chi}^0_r}, m^2_{\tilde{\nu}_{Rs}}, m^2_{\tilde{\nu}_{La'}})], \quad (19)
\end{aligned}
$$

$$
\begin{aligned}
&\approx 2 v_u K_{aa'} \sum_{b,r}(-1)^b g_b \frac{1}{m_{\tilde{\chi}^0_r}} O_{rb} O_{r4} \\
&\quad\times [M_5^2 f_3(m^2_{\tilde{\chi}^0_r}, m^2_{\tilde{\nu}_{R5}}, m^2_{\tilde{\nu}_L}) - M_6^2 f_3(m^2_{\tilde{\chi}^0_r}, m^2_{\tilde{\nu}_{R6}}, m^2_{\tilde{\nu}_L})], \quad (20)
\end{aligned}
$$

where O_{rb} are the neutralino mixing matrices, $r = 1, \ldots, 4$ denotes the neutralino mass eigenstates, and b can be 1 (bino) or 2 (wino). The function f_3 is defined as

$$
\begin{aligned}
f_3(m_0^2, m_1^2, m_2^2) &= \frac{1}{16\pi^2}\frac{m_0^2}{m_1^2 - m_2^2}\left[\left(1 - \frac{m_0^2}{m_1^2}\right)^{-1}\ln\frac{m_1^2}{m_0^2}\right. \\
&\quad \left. - \left(1 - \frac{m_0^2}{m_2^2}\right)^{-1}\ln\frac{m_2^2}{m_0^2}\right] \quad (21)
\end{aligned}
$$

and is shown on the left panel of Fig. 5, being symmetric with respect to $m_1 \leftrightarrow m_2$ exchange. It is clear that f_3 is largest when m_1 and m_2 are smallest. Furthermore, for fixed m_1, m_2, this function is maximized when $m_0 \sim {\rm Max}(m_1, m_2)$.

Finally, for the pure gaugino case we have no suppressed vertices, but need two LR transitions on the sneutrino line. As shown on the bottom row of Fig. 4, in order to contribute to δM_L, these must combine one LNV and one LNC mass insertion:

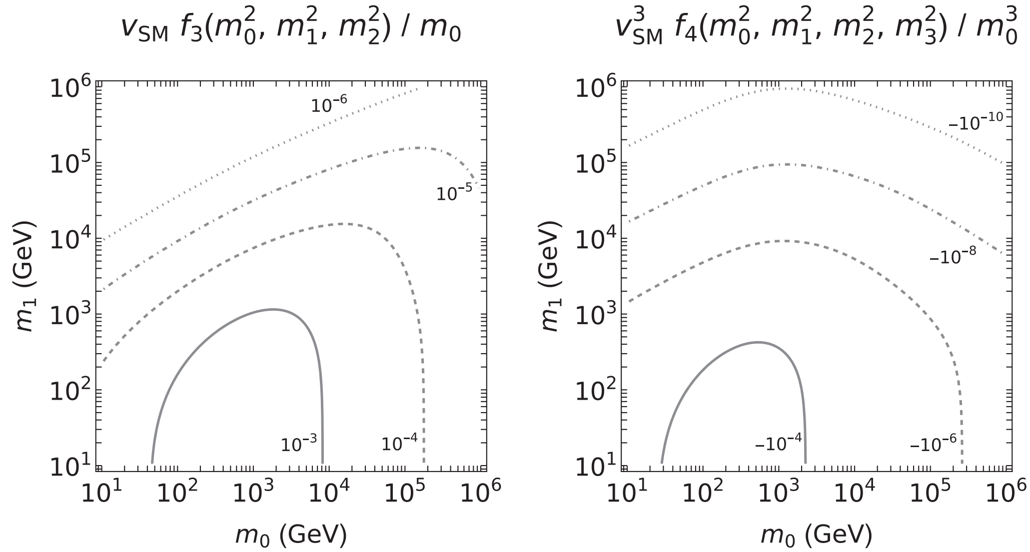

FIG. 5. Mass insertion functions f_3 (left) and f_4 (right), each with a convenient normalization. We set $m_2 = m_3 = 600$ GeV.

$$(\delta M_L^{\rm irr})^{gg}_{aa'} = \frac{v_u^2}{4}\sum_{b,b',s,r}(-1)^{b+b'}g_b g_{b'}\frac{1}{m^3_{\tilde\chi^0_r}}O_{rb}O_{rb'}f_4(m^2_{\tilde\chi^0_r}, m^2_{\tilde\nu_{La}}, m^2_{\tilde\nu_{Rs}}, m^2_{\tilde\nu_{La'}}) \times [(T_\nu^* - \mu^* Y_\nu^* \cot\beta)_{as}(Y_\nu^* M_R^*)_{a's} + (Y_\nu^* M_R^*)_{as}(T_\nu^* - \mu^* Y_\nu^* \cot\beta)_{a's}], \tag{22}$$

$$\approx v_u^2 K_{aa'}(a_\nu - \mu\cot\beta)\sum_{b,b',r}(-1)^{b+b'}g_b g_{b'}\frac{1}{m^3_{\tilde\chi^0_r}}O_{rb}O_{rb'}\times[M_5^2 f_4(m^2_{\tilde\chi^0_r}, m^2_{\tilde\nu_{R5}}, m^2_{\tilde\nu_L}, m^2_{\tilde\nu_L}) - M_6^2 f_4(m^2_{\tilde\chi^0_r}, m^2_{\tilde\nu_{R6}}, m^2_{\tilde\nu_L}, m^2_{\tilde\nu_L})]. \tag{23}$$

The function f_4 follows the general expression:

$$f_n(m_0^2, m_1^2, m_2^2, \ldots, m_{n-1}^2) = \frac{m_0^2}{m_1^2 - m_2^2}[f_{n-1}(m_0^2, m_1^2, m_3^2, \ldots, m_{n-1}^2) - f_{n-1}(m_0^2, m_2^2, m_3^2, \ldots, m_{n-1}^2)], \tag{24}$$

where $n-1$ is the number of mass insertions in the diagram. It is shown on the right panel of Fig. 5, and again is symmetric under exchange of $m_i \leftrightarrow m_j$, $i, j \neq 0$. As with f_3, the function f_4 has larger values for smaller m_i and m_0 around the largest of the m_i.

2. Reducible contributions ($B_\nu \neq 0$)

Once B_ν is different from zero, a new set of loop corrections can enter the game. For this, it is important to assume that the $B_\nu/m^2_{\tilde\nu_R}$ suppression associated with this insertion must not be as strong as the one from Y_ν, allowing diagrams with a larger number of insertions.

Let us start again with the pure Higgsino case, which had negligible irreducible contributions. This time, the self-energy, shown in the top row of Fig. 6, is given by

$$(\delta M_L^{\rm red})^{hh}_{aa'} = \sum_{r,s,s'}\frac{1}{m_{\tilde\chi^0_r}}O_{r4}^2(Y_\nu^*)_{as}(B_\nu^*)_{ss'}(Y_\nu^*)_{a's'}f_3(m^2_{\tilde\chi^0_r}, m^2_{\tilde\nu_{Rs}}, m^2_{\tilde\nu_{Rs'}}), \tag{25}$$

$$\approx 2K_{aa'}b_\nu\sum_r\frac{1}{m_{\tilde\chi^0_r}}O_{r4}^2[M_5^2 f_3(m^2_{\tilde\chi^0_r}, m^2_{\tilde\nu_{R5}}, m^2_{\tilde\nu_{R5}}) - M_6^2 f_3(m^2_{\tilde\chi^0_r}, m^2_{\tilde\nu_{R6}}, m^2_{\tilde\nu_{R6}})]. \tag{26}$$

The loop function f_3 is shown in Eq. (21), and illustrated in the left panel of Fig. 5.

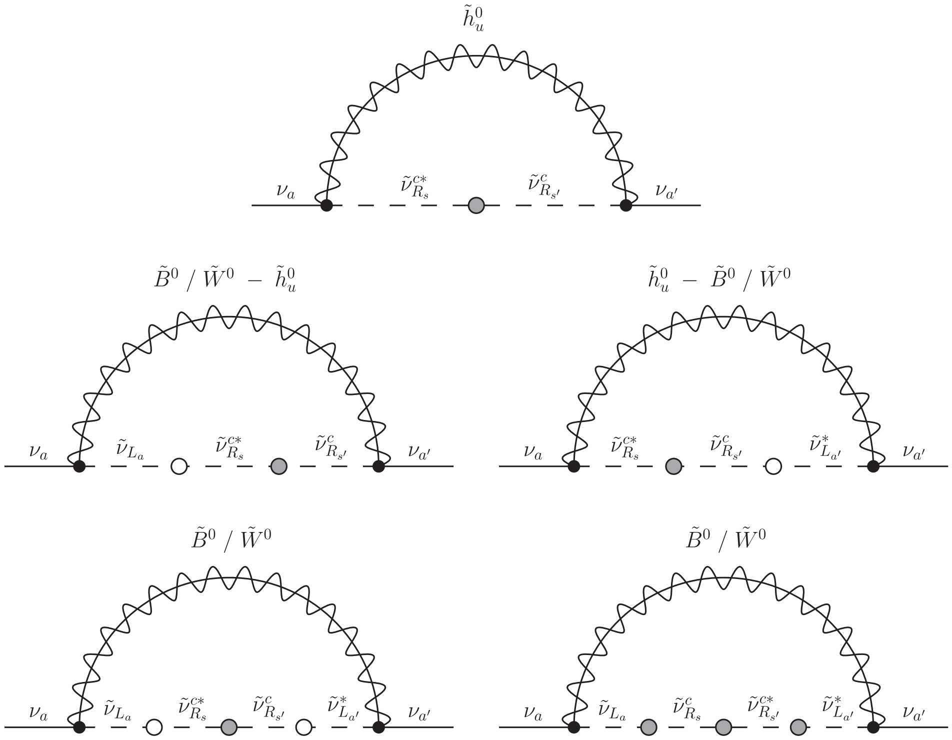

FIG. 6. Reducible mass insertions. In all cases, gray (white) blobs indicate LNV (LNC) insertions. Top: pure Higgsino case. Center: gaugino-Higgsino case. Bottom: pure gaugino case.

For the gaugino-Higgsino correction, we now can have two insertions, one of them being a LR transition that is LNC, and then the RR insertion from B_ν. This can be seen on the center row of Fig. 6, leading to

$$(\delta M_L^{\rm red})_{aa'}^{gh} = \frac{v_u}{4}\sum_{b,s,s',r}(-1)^b g_b \frac{1}{m_{\tilde{\chi}_r^0}^3} O_{rb}O_{r4}[(T_\nu^* - \mu^* \cot\beta Y_\nu^*)_{as'}(B_\nu^*)_{ss'}(Y_\nu^*)_{a's} f_4(m_{\tilde{\chi}_r^0}^2, m_{\tilde{\nu}_{La}}^2, m_{\tilde{\nu}_{Rs'}}^2, m_{\tilde{\nu}_{Rs}}^2)$$
$$+ (Y_\nu^*)_{as}(B_\nu^*)_{s's}(T_\nu^* - \mu^* \cot\beta Y_\nu^*)_{a's'} f_4(m_{\tilde{\chi}_r^0}^2, m_{\tilde{\nu}_{Rs}}^2, m_{\tilde{\nu}_{Rs'}}^2, m_{\tilde{\nu}_{La'}}^2)], \tag{27}$$

$$\approx v_u K_{aa'}(a_\nu - \mu\cot\beta) b_\nu \sum_{b,r}(-1)^b g_b \frac{1}{m_{\tilde{\chi}_r^0}^3} O_{rb}O_{r4}[M_5^2 f_4(m_{\tilde{\chi}_r^0}^2, m_{\tilde{\nu}_L}^2, m_{\tilde{\nu}_{R5}}^2, m_{\tilde{\nu}_{R5}}^2) - M_6^2 f_4(m_{\tilde{\chi}_r^0}^2, m_{\tilde{\nu}_L}^2, m_{\tilde{\nu}_{R6}}^2, m_{\tilde{\nu}_{R6}}^2)]. \tag{28}$$

Here, the loop function f_4 is deduced from Eq. (24) and shown on the right panel of Fig. 5.

Finally, following the bottom row of Fig. 6, the pure gaugino loops have three mass insertions, with two LR transitions in addition to the B_ν insertion:

$$(\delta M_L^{\rm red})_{aa'}^{gg} = \frac{v_u^2}{8}\sum_{b,b',s,s',r}(-1)^{b+b'} g_b g_{b'} \frac{1}{m_{\tilde{\chi}_r^0}^5} O_{rb}O_{rb'} f_5(m_{\tilde{\chi}_r^0}^2, m_{\tilde{\nu}_{La}}^2, m_{\tilde{\nu}_{Rs}}^2, m_{\tilde{\nu}_{Rs'}}^2, m_{\tilde{\nu}_{La'}}^2)$$
$$\times [(Y_\nu^* M_R^*)_{as}(B_\nu)_{ss'}(Y_\nu^* M_R^*)_{a's'} + (T_\nu^* - \mu^* \cot\beta Y_\nu^*)_{as}(B_\nu^*)_{ss'}(T_\nu^* - \mu^* \cot\beta Y_\nu^*)_{a's'}], \tag{29}$$

$$\approx \frac{v_u^2}{4} K_{aa'} b_\nu \sum_{b,b',r}(-1)^{b+b'} g_b g_{b'} \frac{1}{m_{\tilde{\chi}_r^0}^5} O_{rb}O_{rb'}[M_5^2(M_5^2 + (a_\nu - \mu\cot\beta)^2) f_5(m_{\tilde{\chi}_r^0}^2, m_{\tilde{\nu}_{R5}}^2, m_{\tilde{\nu}_{R5}}^2, m_{\tilde{\nu}_L}^2, m_{\tilde{\nu}_L}^2)$$
$$- M_6^2(M_6^2 + (a_\nu - \mu\cot\beta)^2) f_5(m_{\tilde{\chi}_r^0}^2, m_{\tilde{\nu}_{R6}}^2, m_{\tilde{\nu}_{R6}}^2, m_{\tilde{\nu}_L}^2, m_{\tilde{\nu}_L}^2)]. \tag{30}$$

As before, the function f_5 is calculated following Eq. (24), following the general properties outlined earlier for f_3 and f_4.

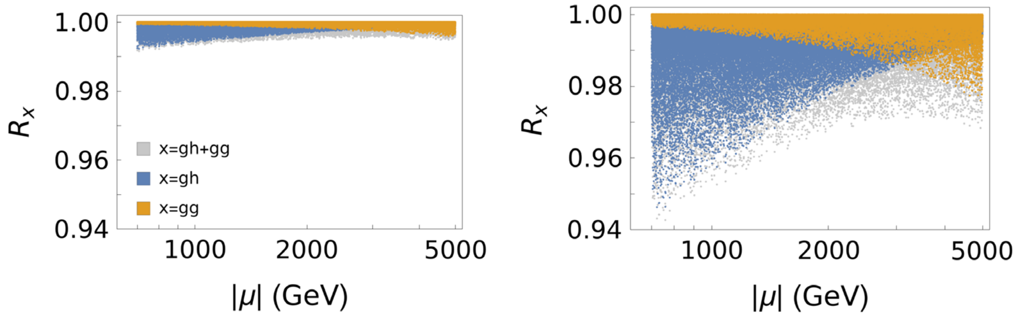

FIG. 7. R_x parameter for increasing $|\mu|$, with $M_5 = 40$ (200) GeV on the left (right). Gaugino-Higgsino (pure gaugino) cancellations are shown in blue (orange), with combined contribution in gray.

IV. SEARCHING FOR CANCELLATIONS

The main purpose of this work is to find under what conditions can one have large LNV terms while keeping loop corrections under control, avoiding the need for fine-tuning in the neutrino sector. Since we know that the non-SUSY contributions are very similar to those in the standard seesaw, it is necessary to have a cancellation featuring the sneutrino loops. In fact, presenting this SUSY screening was the main motivation of [26], where it was suggested that the nonrenormalization theorems could enforce such a result. So, in the following we concentrate on characterizing the region of the parameter space guaranteeing destructive interference for both reducible and irreducible corrections.

A. Irreducible contributions

In order to understand how these corrections affect neutrino masses, let us first assume that $\tilde{\nu}_{R5}$ and $\tilde{\nu}_{R6}$ are degenerate. In this limit, all SUSY loop diagrams are proportional to $(Y_\nu^* M_R^* Y_\nu^\dagger)_{aa'} = 2K_{aa'}(M_5^2 - M_6^2)$. Then, if both neutrinos and sneutrinos are independently degenerate, one should expect all loop corrections to vanish, and thus with no fine-tuning on light neutrino masses. We attribute this, on the one hand, to the cancellation of additional LNV terms on the neutrino side, and, on the other hand, to the fact that in the unbroken SUSY limit a mass degeneracy for neutrinos would also imply degenerate sneutrino masses.

If $\Delta M_{65} \neq 0$, then both SUSY and non-SUSY contributions can be large, so we need them to interfere destructively. As a first step, we have confirmed the result of [26] in their SUSY-conserving limit, where M_{SUSY}, $\mu \to 0$ and $\tan\beta \to 1$. Here, the only nonvanishing SUSY contribution is the gaugino-Higgsino $(\delta M_L^{\mathrm{irr}})^{gh}$, which precisely cancels $(\delta M_L)^{\mathrm{2HDM}}$.

However, once one considers broken SUSY, the cancellations become inefficient, with $(\delta M_L^{\mathrm{irr}})^{gh}$ being subdominant with respect to $(\delta M_L)^{\mathrm{2HDM}}$. We find destructive interference to be more likely if $m_{\tilde{L}}$, $m_{\tilde{\nu}_R}$, $M_{1,2}$, and μ are relatively light, or if heavy neutrino masses are close to the SUSY scale. However, due to the lack of experimental evidence in favor of SUSY, the sparticles must be heavy, making it very difficult to have large cancellations involving $(\delta M_L^{\mathrm{irr}})^{gh}$ in the region accessible to heavy neutrino searches.

An important point to consider is that, once SUSY is broken, the pure gaugino $(\delta M_L^{\mathrm{irr}})^{gg}$ can play an important role. For $a_\nu = 0$, we find that the overall sign of this contribution depends on the relative sign between μ and $M_{1,2}$. In the following, we choose $\mu < 0$ and $M_{1,2} > 0$, which guarantees destructive interference with $(\delta M_L)^{\mathrm{2HDM}}$. In this case, a light SUSY spectrum is again favored, but can now be enhanced by large $|\mu|$. This is also the case when a_ν is large and positive.

In order to illustrate our findings, we define $R_x = 1 + [(\delta M_L^{\mathrm{irr}})^x / (\delta M_L)^{\mathrm{2HDM}}]$ as a measure of the amount of cancellation possible between the SUSY and non-SUSY loop corrections, with $x = gh + gg, gh, gg$. Notice that the flavor structure of $(\delta M_L^{\mathrm{irr}})^x$ and $(\delta M_L)^{\mathrm{2HDM}}$ effectively cancels, leaving R_x without flavor indices.

A scatter plot of R_x as a function of $|\mu|$ is shown in Fig. 7, for two values of heavy neutrino mass, M_5. In the scan we have varied $-\mu, M_2, m_{\tilde{L}}, m_{\tilde{\nu}}$ logarithmically between 700 and 5000 GeV but allowing a soft mass $m_{\tilde{\nu}}$ as low as 0.1 GeV. We have set $M_1 = M_2/2$ and $a_\nu = 0$. Results are not strongly sensitive to ΔM_{65}, nor any other parameter. In the figure we confirm that cancellations are driven by $(\delta M_L^{\mathrm{irr}})^{gh}$ for small $|\mu|$ and taken over by $(\delta M_L^{\mathrm{irr}})^{gg}$ as $|\mu|$ grows. The combined contributions are relevant for intermediate values of $|\mu|$. Here, we confirm that the SUSY contribution cannot lead to strong cancellations any more, being less than 1% (5%) for $M_h = 40$ (200) GeV, and thus it cannot solve the fine-tuning problem.

It is then of interest to understand the results of [26], who were able to relax constraints on LNV within their radiative inverse seesaw. Even though their setup is somewhat different from ours, the cancellation mechanisms are the same, and should be comparable regardless of the exact scenario in use. In order to shine light on the matter, we plot in Fig. 8 the maximum ΔM_{65} allowed by requiring the full (SUSY + non-SUSY) loop corrections to be less than 50%

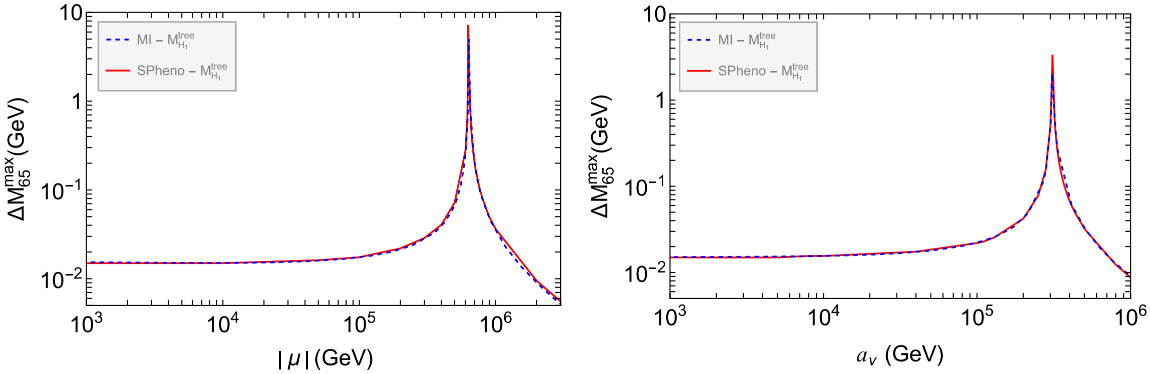

FIG. 8. Maximum allowed ΔM_{65} as a function of $|\mu|$ (a_ν) on the left (right), for the SUSY spectrum considered in [26], with $\tan\beta = 2$. We set $\gamma_{56} = 8$, such that $|U_{\mu 5}|^2 = 1.3 \times 10^{-7}$.

as a function of $|\mu|$ or a_ν. The rest of the parameters are set as in Table II in [26]. Within the figure, we show curves obtained with our mass-insertion formulas, compared with those from SPheno [56,57], which performs the exact calculation using the tree-level Higgs mass.[6]

The first thing we notice is that, as verified by SPheno, the mass-insertion approximation holds very well, even for extremely large $|\mu|$ and a_ν. In addition, we also find that there exist values for both parameters where SUSY and non-SUSY contributions cancel, allowing for a very large ΔM_{65}. These are in the ballpark of the corresponding values reported in [26]. The explanation for this is that $(\delta M_L^{\rm irr})^{gg}$ has become very large, enhanced by either $|\mu|$ or a_ν, and can cancel $(\delta M_L)^{\rm 2HDM}$, thus relaxing the LNV constraint on ΔM_{65}. In fact, we see that the maximum ΔM_{65} decreases considerably after this cancellation, meaning that from this point $(\delta M_L^{\rm irr})^{gg}$ not only cancels but exceeds $(\delta M_L)^{\rm 2HDM}$, needing an even smaller ΔM_{65} to be under control.

What we conclude is that, in order to achieve the required cancellation, it is essential to select very precise values for either $|\mu|$ or a_ν, greatly enhancing the pure gaugino contribution. Unfortunately, comparing this result with Fig. 1, it can be argued that in this scenario the fine-tuning of the neutrino sector has been transferred to the SUSY sector, although this time without a symmetry such as LN to justify it.

Apart from this issue, we believe the large $|\mu|, a_\nu$ solutions have additional problems, which need to be addressed. Regarding $|\mu|$, the SUSY minimization conditions would lead to a second situation with large fine-tuning, as the soft Higgs masses would need to have very special values to trigger electroweak symmetry breaking and reproduce the observed Z mass simultaneously. It is likely this would also convey very large loop corrections to the light Higgs mass, leading to a third fine-tuning. On the other hand, for a_ν, it was argued in [64] that in order to avoid charge-breaking minima, one had to satisfy

$$(a_\nu + M_R)^2 \le 3(m_{H_u}^2 + |\mu|^2 + m_{\tilde{L}}^2 + m_{\tilde{\nu}_R}^2 + M_R^2 + B_\nu), \quad (31)$$

which is unlikely to hold given the benchmark spectrum. Thus, we do not consider the cancellations featured in [26] to be a generic feature of the ν_RMSSM, but to rather require additional ingredients beyond the simple structure of the model.

There does exist an alternative way of slightly improving the cancellations that, although inelegant,[7] does not require such large parameters. A direct inspection of Eqs. (20) and (23) shows that the $\tilde{\nu}_{R5}$ and $\tilde{\nu}_{R6}$ terms have opposite signs, meaning that the SUSY contribution is diminished when R-sneutrinos are degenerate. Then, if R-sneutrino masses are different, and if one of these is very large such that the corresponding R-sneutrino is decoupled, the SUSY contribution is maximized. However, the choice of which R-sneutrino needs to be decoupled depends on the neutrino sector. For example, we find that if $M_6 > M_5$, then it is $\tilde{\nu}_{R5}$ who must be decoupled in order to guarantee destructive interference (with $\mu < 0$ as before). In other words, the R-sneutrino hierarchy needs to be inverted with respect to the one for heavy neutrinos.

Given the properties of the loop functions, the most effective hierarchy leading to cancellations is $m_{\tilde{\nu}_{R6}} \ll m_{\tilde{L}} < -\mu, M_1, M_2 \ll m_{\tilde{\nu}_{R5}}$. This suggests a spectrum similar to that of [30,65], which avoided LHC constraints and provided a R-sneutrino dark matter candidate [64]. Considering this hierarchy, we show R_{gh+gg} as a function of $m_{\tilde{\nu}_{R6}}$ on the left panel of Fig. 9, for different neutrino mass splittings. The model parameters are $m_A = 1.1$ TeV,

[6]The model was implemented using SARAH [58–63].

[7]It is very unlikely that a high-scale model would provide such a spectrum after running the RGEs. Also, even in the case of a moderate splitting, the RGEs would generate off-diagonal soft terms, likely leading to problems with lepton flavor violating processes.

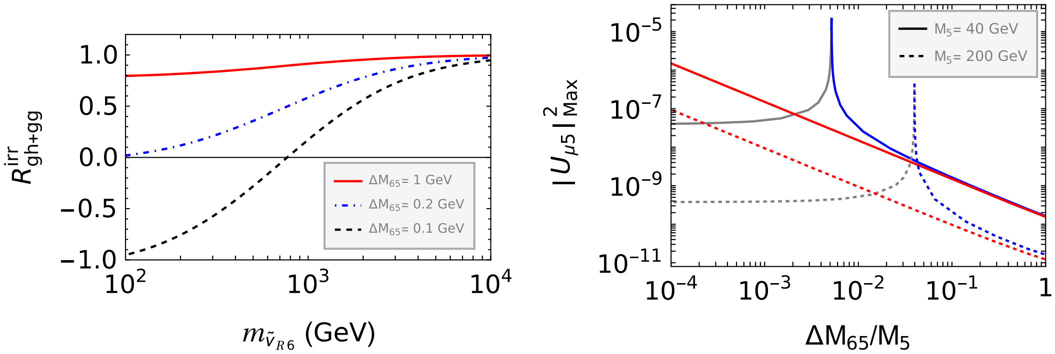

FIG. 9. Left: dependence of R_{gh+gg} with $m_{\tilde{\nu}_{R6}}$, for several values of ΔM_{65}. Heavy neutrino mass is set to $M_5 = 40$ GeV. Right: maximum allowed value of $|U_{\mu5}|^2$, as a function of $\Delta M_{65}/M_5$, for two values of M_5. Limits on for the standard seesaw are shown in red. Blue and gray lines show limits for the spectrum described in the text. For gray lines, the SUSY contribution is larger the one from 2HDM.

$\tan\beta = 8$, $m_{\tilde{L}} = 500\,\text{GeV}$, $M_2 = 750$ GeV, $M_1 = M_2/2$, $\mu = -1$ TeV, and $a_\nu = 0$. The figure shows that, for a fixed ΔM_{65}, the value of R_{gh+gg} increases with $m_{\tilde{\nu}_{R6}}$. Thus, cancellations are stronger for $m_{\tilde{\nu}_{R6}}$ closest to the corresponding heavy neutrino mass (i.e., vanishing soft mass). Moreover, contrary to the degenerate case, the efficiency of the cancellation does depend on the heavy neutrino mass splitting, with smaller values of R_{gh+gg} for smaller ΔM_{65}. The reason is that the full SUSY contribution no longer depends on the neutrino splitting, meaning that reducing ΔM_{65} decreases only $(\delta M_L)^{\text{2HDM}}$, thus leading to lower R_{gh+gg}. Nevertheless, contrary to the degenerate case, this time the destructive interference can be substantial for moderate values of $|\mu|$, in some cases having the SUSY contribution exceeding the non-SUSY part ($R_{gh+gg} < 0$).

The right panel of Fig. 9 compares the maximum $|U_{\mu5}|^2$ of the standard seesaw with that on our scenario, for the aforementioned spectrum. The bounds for the standard seesaw are shown in red, while the corresponding constraints for our model are shown in blue. Even though one can see a non-negligible relaxation of the bounds for small $\Delta M_{65}/M_5$, we find this effect vanishes when the splitting is large. Thus, we conclude that even for the nondegenerate case, SUSY does not relax the fine-tuning associated to heavy neutrinos with large mass splitting and mixing.

As a final comment, the figure also shows gray curves for very small ΔM_{65}, which place bounds much more stringent than those of the standard seesaw. Here, we find the SUSY contribution to be dominant, corresponding to negative R_{gh+gg}. To avoid these constraints one needs to take a heavier SUSY spectrum, in particular, larger $m_{\tilde{\nu}_{R6}}$ or $m_{\tilde{L}}$.

B. Reducible contributions

Let us briefly comment on the three types of reducible contributions in our benchmark scenario, for degenerate sneutrinos and $a_\nu = 0$, focusing on how to guarantee a cancellation with the non-SUSY part. First, we find that regardless of the spectrum, and for both signs of μ, the gaugino-gaugino correction in Eq. (30) gives destructive interference as long as $b_\nu < 0$.

The gaugino-Higgsino loop of Eq. (28) also leads to cancellations for $b_\nu < 0$, as long as $\mu < 0$. If μ is positive, then we find that the sign of the correction depends on the spectrum. However, we will not consider this possibility, as $\mu < 0$ is also favored by the irreducible gaugino-gaugino contribution.

As can be seen in Eq. (26), the Higgsino-Higgsino correction does not depend on $m_{\tilde{L}}$. Again concentrating on negative μ, we find destructive interference for $b_\nu < 0$ if $|\mu|$ is large. If $|\mu|$ is small, then there exists a change in sign, requiring $b_\nu > 0$ for cancellations. However, the latter possibility is in conflict with the other reducible corrections, which require $b_\nu < 0$.

Thus, if we want all reducible and irreducible corrections to work together in canceling the non-SUSY contribution, we need μ to be large and negative, as well as a negative b_ν. In order to illustrate its behavior we show, on the left panel of Fig. 10, the corresponding $R^{\text{red}}_{gg+gh+hh}$ considering only the reducible contribution, as a function of $|\mu|$ and $m_{\tilde{L}}$. Here, we have taken negative μ, and varied $M_2 = 2M_1$ between 700 and 5000 GeV. Since effects are maximized for small $m_{\tilde{\nu}}$, we have set this parameter equal to 0.5 GeV and, in order to avoid tachyonic states, set $b_\nu = M_5 - 5$ GeV.[8] Results are shown only for $M_5 = 200$ GeV.

In all points, we find that the gaugino-gaugino contribution dominates the correction, usually followed by gaugino-Higgsino and then Higgsino-Higgsino contributions. We also find that the dependence on ΔM_{65} practically cancels with that of the non-SUSY part, so our results can be taken independent of the heavy neutrino mass splitting. However, within the evaluated parameter space, the

[8] Even though this is a relatively large value of b_ν, we have checked that our results coincided reasonably well with SPheno.

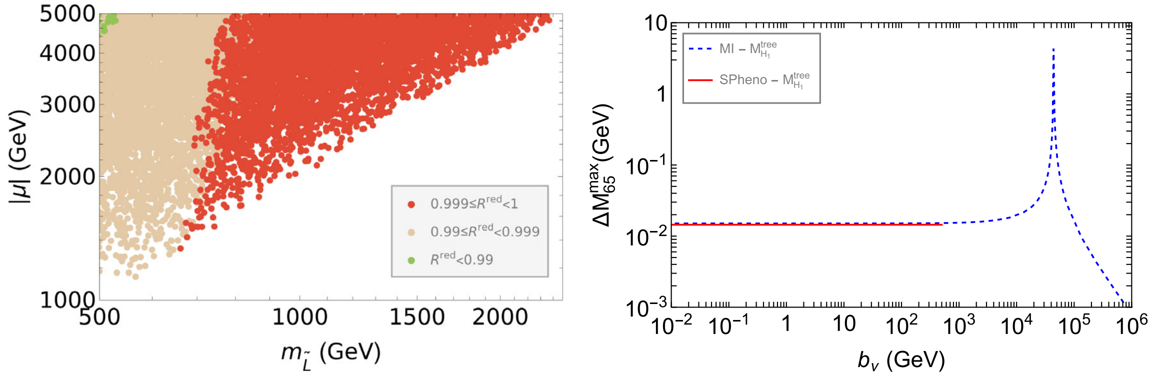

FIG. 10. Left: values of $R^{\rm red}_{gg+gh+hh}$ parameter for different values of $m_{\tilde{L}}$ and $|\mu|$, with $M_5 = 200$ GeV. Right: maximum allowed ΔM_{65} as a function of b_ν, for the SUSY spectrum considered in [26], with $\tan\beta = 2$. We set $\gamma_{56} = 8$, such that $|U_{\mu 5}|^2 = 1.3 \times 10^{-7}$.

cancellation is hardly above 1%, which happens for very large $|\mu|$ and very small $m_{\tilde{L}}$. The situation is worse for smaller M_5. When compared to the corresponding irreducible contributions, we find that the reducible part never rises above 0.6% of the latter. Thus, we consider reducible contributions not worth considering any further.

Similarly to the irreducible case, the work in [26] claims that one can find values of b_ν of $\mathcal{O}(0.1\ \text{GeV})$ that again cancel the non-SUSY loops. This time, we have not been able to reproduce their result. We show our attempt on the right panel of Fig. 10, where we again plot the maximum ΔM_{65} in their benchmark scenario (note they use $\mu, b_\nu > 0$). We do not find any cancellation around their expected value, coinciding with the prediction from SPheno. Thus, it is possible that the b_ν-based screening is a feature of models with radiative light neutrino masses. As a final remark, within the mass-insertion method, we again found that very large values of b_ν could be tuned in order to have the necessary destructive interference. These would work for $\mu > 0$, and would be dominated by reducible Higgsino-Higgsino loops. However, one should not expect the mass insertion method to hold for such large values of b_ν, and in any case, when contrasted with SPheno, we found that these would lead to tachyonic sneutrino states.

V. DISCUSSION

In this work we have briefly reviewed the problem of large loop corrections to light neutrino masses in the type-I seesaw model, which can be present in scenarios where the active-heavy mixing is large. It is well known that a good way of avoiding the problem is by assigning to the model a slightly broken LN symmetry, which forces the heavy neutrinos to appear as pseudo-Dirac states. This, however, can constrain LNV signals from appearing in collider searches.

We then evaluated a work appearing some years ago, which proposed considering a supersymmetric extension to the model as a way of keeping loop corrections under control. This study was motivated by the fact that in unbroken SUSY the quantum corrections to terms in the superpotential are canceled, leading to the hope than in the broken case a soft SUSY screening effect would follow. The expectation from this was that larger LNV parameters would be allowed on the neutrino sector, reflected on larger heavy neutrino mass splittings. This, in turn, would better motivate searches for LNV phenomena associated to a single heavy neutrino at colliders.

We thus performed a detailed analysis of the two irreducible and three reducible SUSY contributions to the loop corrected masses. We determined the regions of parameter space guaranteeing cancellations between the latter and the non-SUSY loops, concentrating on heavy neutrino mass ranges accessible to current collider experiments.

To summarize, we found the largest SUSY quantum corrections to be the irreducible ones. For the case of degenerate sneutrinos, with parameters under the TeV scale, we found no significant screening effect. We did corroborate that the pure gaugino loops could cancel the non-SUSY contributions for extremely large values of $|\mu|$ and a_ν, but argued that doing so could cause problems in other sectors of the model. We also presented a nonelegant scenario with very nondegenerate sneutrinos, and found that the screening could be more efficient without needing too large $|\mu|$ or a_ν. However, regardless of this, the relaxation of constraints on LNV was very mild.

It must be noted that none of the cases above, where the cancellations could be efficient, arises as a consequence of nonrenormalization theorems. The only SUSY screening contribution that does not rely on SUSY breaking, and thus could be attributed to the theorems, is the irreducible gaugino-Higgsino loop which, as we have shown, only dominates for small $|\mu|$. None of the cases with efficient cancellations rely on this correction. Instead, they all need very specific values for the parameters, suggesting that what we are observing is a transfer of fine-tuning from the neutrino sector to the SUSY sector of the model. In our opinion, even though SUSY screening does sound appealing in principle, in practice it does not seem reasonable to bring in the whole supersymmetric framework to address this issue.

ACKNOWLEDGMENTS

The authors would like to thank Werner Porod for thorough discussions and a careful reading of the draft. We also would like to thanks Apostolos Pilaftsis for clarifications regarding their work. We acknowledge funding by the *Dirección de Gestión de la Investigación* at PUCP, through Grant No. DGI-2021-C-0020, and have been also been supported by the DAAD-CONCYTEC Project No. 131-2017-FONDECYT. O. S. N. was funded by Grant No. 236-2015-FONDECYT.

[1] Peter Minkowski, $\mu \to e\gamma$ at a rate of one out of 1-billion muon decays?, Phys. Lett. **67B**, 421 (1977).

[2] Murray Gell-Mann, Pierre Ramond, and Richard Slansky, Complex spinors and unified theories, Conf. Proc. C **790927**, 315 (1979).

[3] Tsutomu Yanagida, Horizontal symmetry and masses of neutrinos, Conf. Proc. C **7902131**, 95 (1979).

[4] Rabindra N. Mohapatra and Goran Senjanovic, Neutrino Mass and Spontaneous Parity Violation, Phys. Rev. Lett. **44**, 912 (1980).

[5] J. Schechter and J. W. F. Valle, Neutrino masses in $\mathrm{SU}(2) \times \mathrm{U}(1)$ theories, Phys. Rev. D **22**, 2227 (1980).

[6] Anupama Atre, Tao Han, Silvia Pascoli, and Bin Zhang, The search for heavy Majorana neutrinos, J. High Energy Phys. 05 (2009) 030.

[7] Frank F. Deppisch, P. S. Bhupal Dev, and Apostolos Pilaftsis, Neutrinos and collider physics, New J. Phys. **17**, 075019 (2015).

[8] Asli M. Abdullahi *et al.*, The present and future status of heavy neutral leptons, J. Phys. G **50**, 020501 (2022).

[9] J. A. Casas and A. Ibarra, Oscillating neutrinos and $\mu \to e, \gamma$, Nucl. Phys. **B618**, 171 (2001).

[10] A. Ibarra, E. Molinaro, and S. T. Petcov, TeV scale see-saw mechanisms of neutrino mass generation, the Majorana nature of the heavy singlet neutrinos and $(\beta\beta)_{0\nu}$-decay, J. High Energy Phys. 09 (2010) 108.

[11] D. Aristizabal Sierra and Carlos E. Yaguna, On the importance of the 1-loop finite corrections to seesaw neutrino masses, J. High Energy Phys. 08 (2011) 013.

[12] Manimala Mitra, Goran Senjanovic, and Francesco Vissani, Neutrinoless double beta decay and heavy sterile neutrinos, Nucl. Phys. **B856**, 26 (2012).

[13] J. Lopez-Pavon, S. Pascoli, and Chan-fai Wong, Can heavy neutrinos dominate neutrinoless double beta decay?, Phys. Rev. D **87**, 093007 (2013).

[14] Alberto M. Gago, Pilar Hernández, Joel Jones-Pérez, Marta Losada, and Alexander Moreno Briceño, Probing the type I seesaw mechanism with displaced vertices at the LHC, Eur. Phys. J. C **75**, 470 (2015).

[15] J. Lopez-Pavon, E. Molinaro, and S. T. Petcov, Radiative corrections to light neutrino masses in low scale type I seesaw scenarios and neutrinoless double beta decay, J. High Energy Phys. 11 (2015) 030.

[16] P. Hernández, J. Jones-Pérez, and O. Suarez-Navarro, Majorana vs pseudo-dirac neutrinos at the ILC, Eur. Phys. J. C **79**, 220 (2019).

[17] Patrick D. Bolton, Frank F. Deppisch, and P. S. Bhupal Dev, Neutrinoless double beta decay versus other probes of heavy sterile neutrinos, J. High Energy Phys. 03 (2020) 170.

[18] G. C. Branco, W. Grimus, and L. Lavoura, The seesaw mechanism in the presence of a conserved lepton number, Nucl. Phys. **B312**, 492 (1989).

[19] Mikhail Shaposhnikov, A possible symmetry of the nuMSM, Nucl. Phys. **B763**, 49 (2007).

[20] Jörn Kersten and Alexei Yu. Smirnov, Right-handed neutrinos at CERN LHC and the mechanism of neutrino mass generation, Phys. Rev. D **76**, 073005 (2007).

[21] M. B. Gavela, T. Hambye, D. Hernandez, and P. Hernandez, Minimal flavour seesaw models, J. High Energy Phys. 09 (2009) 038.

[22] Marco Drewes, Juraj Klarić, and Philipp Klose, On lepton number violation in heavy neutrino decays at colliders, J. High Energy Phys. 11 (2019) 032.

[23] Jean-Loup Tastet, Oleg Ruchayskiy, and Inar Timiryasov, Reinterpreting the ATLAS bounds on heavy neutral leptons in a realistic neutrino oscillation model, J. High Energy Phys. 12 (2021) 182.

[24] Asmaa Abada, Pablo Escribano, Xabier Marcano, and Gioacchino Piazza, Collider searches for heavy neutral leptons: Beyond simplified scenarios, Eur. Phys. J. C **82**, 1030 (2022).

[25] Enrique Fernández-Martínez, Xabier Marcano, and Daniel Naredo-Tuero, HNL mass degeneracy: Implications for low-scale seesaws, LNV at colliders and leptogenesis, J. High Energy Phys. 03 (2023) 057.

[26] Pablo Candia da Silva and Apostolos Pilaftsis, Radiative neutrino masses in the ν_RMSSM, Phys. Rev. D **102**, 095013 (2020).

[27] Marcus T. Grisaru, W. Siegel, and M. Rocek, Improved methods for supergraphs, Nucl. Phys. **B159**, 429 (1979).

[28] Nathan Seiberg, Naturalness versus supersymmetric nonrenormalization theorems, Phys. Lett. B **318**, 469 (1993).

[29] A. Donini, P. Hernandez, J. Lopez-Pavon, M. Maltoni, and T. Schwetz, The minimal $3+2$ neutrino model versus oscillation anomalies, J. High Energy Phys. 07 (2012) 161.

[30] Nhell Cerna-Velazco, Thomas Faber, Joel Jones-Perez, and Werner Porod, Constraining sleptons at the LHC in a supersymmetric low-scale seesaw scenario, Eur. Phys. J. C **77**, 661 (2017).

[31] J. Jones-Pérez, J. Masias, and J. D. Ruiz-Álvarez, Search for long-lived heavy neutrinos at the LHC with a VBF trigger, Eur. Phys. J. C **80**, 642 (2020).

[32] W. Grimus and H. Neufeld, Radiative neutrino masses in an $SU(2) \times U(1)$ model, Nucl. Phys. **B325**, 18 (1989).

[33] Apostolos Pilaftsis, Radiatively induced neutrino masses and large Higgs neutrino couplings in the standard model with Majorana fields, Z. Phys. C **55**, 275 (1992).

[34] Walter Grimus and Luis Lavoura, One-loop corrections to the seesaw mechanism in the multi-Higgs-doublet standard model, Phys. Lett. B **546**, 86 (2002).

[35] Piotr H. Chankowski and Zbigniew Pluciennik, Renormalization group equations for seesaw neutrino masses, Phys. Lett. B **316**, 312 (1993).

[36] K. S. Babu, Chung Ngoc Leung, and James T. Pantaleone, Renormalization of the neutrino mass operator, Phys. Lett. B **319**, 191 (1993).

[37] Stefan Antusch, Jörn Kersten, Manfred Lindner, Michael Ratz, and Michael Andreas Schmidt, Running neutrino mass parameters in see-saw scenarios, J. High Energy Phys. 03 (2005) 024.

[38] M. Bustamante, A. M. Gago, and Joel Jones Perez, SUSY renormalization group effects in ultra high energy neutrinos, J. High Energy Phys. 05 (2011) 133.

[39] K. Sashikanta Singh, Subhankar Roy, and N. Nimai Singh, Stability of neutrino parameters and self-complementarity relation with varying SUSY breaking scale, Phys. Rev. D **97**, 055038 (2018).

[40] M. Hirsch, T. Kernreiter, J. C. Romao, and Albert Villanova del Moral, Minimal supersymmetric inverse seesaw: Neutrino masses, lepton flavour violation and LHC phenomenology, J. High Energy Phys. 01 (2010) 103.

[41] W. Grimus and H. Neufeld, Three neutrino mass spectrum from combining seesaw and radiative neutrino mass mechanisms, Phys. Lett. B **486**, 385 (2000).

[42] Alejandro Ibarra and Cristoforo Simonetto, Understanding neutrino properties from decoupling right-handed neutrinos and extra Higgs doublets, J. High Energy Phys. 11 (2011) 022.

[43] Darius Jurciukonis, Thomas Gajdosik, and Andrius Juodagalvis, Seesaw neutrino masses with a second Higgs doublet added (2015), arXiv:1507.03459.

[44] W. Grimus and M. Löschner, Renormalization of the multi-Higgs-doublet standard model and one-loop lepton mass corrections, J. High Energy Phys. 11 (2018) 087.

[45] D. Jurčiukonis, T. Gajdosik, and A. Juodagalvis, Seesaw neutrinos with one right-handed singlet field and a second Higgs doublet, J. High Energy Phys. 11 (2019) 146.

[46] Georges Aad *et al.*, Search for Heavy Higgs Bosons Decaying into Two Tau Leptons with the ATLAS Detector Using pp Collisions at $\sqrt{s} = 13$ TeV, Phys. Rev. Lett. **125**, 051801 (2020).

[47] Georges Aad *et al.*, Search for charged Higgs bosons decaying into a top quark and a bottom quark at $\sqrt{s} = 13$ TeV with the ATLAS detector, J. High Energy Phys. 06 (2021) 145.

[48] Georges Aad *et al.*, Combined measurements of Higgs boson production and decay using up to 80 fb^{-1} of proton-proton collision data at $\sqrt{s} = 13$ TeV collected with the ATLAS experiment, Phys. Rev. D **101**, 012002 (2020).

[49] Athanasios Dedes, Howard E. Haber, and Janusz Rosiek, Seesaw mechanism in the sneutrino sector and its consequences, J. High Energy Phys. 11 (2007) 059.

[50] Wolfgang Gregor Hollik, Radiative generation of neutrino mixing: Degenerate masses and threshold corrections, Phys. Rev. D **91**, 033001 (2015).

[51] F. Gabbiani, E. Gabrielli, A. Masiero, and L. Silvestrini, A complete analysis of FCNC and CP constraints in general SUSY extensions of the standard model, Nucl. Phys. **B477**, 321 (1996).

[52] Mikolaj Misiak, Stefan Pokorski, and Janusz Rosiek, Supersymmetry and FCNC effects, Adv. Ser. Dir. High Energy Phys. **15**, 795 (1998).

[53] J. Hisano and Daisuke Nomura, Solar and atmospheric neutrino oscillations and lepton flavor violation in supersymmetric models with the right-handed neutrinos, Phys. Rev. D **59**, 116005 (1999).

[54] Guy Raz, The mass insertion approximation without squark degeneracy, Phys. Rev. D **66**, 037701 (2002).

[55] A. Dedes, M. Paraskevas, J. Rosiek, K. Suxho, and K. Tamvakis, Mass insertions vs. mass eigenstates calculations in flavour physics, J. High Energy Phys. 06 (2015) 151.

[56] Werner Porod, SPheno, A program for calculating supersymmetric spectra, SUSY particle decays and SUSY particle production at e+ e- colliders, Comput. Phys. Commun. **153**, 275 (2003).

[57] W. Porod and F. Staub, SPheno 3.1: Extensions including flavour, CP-phases and models beyond the MSSM, Comput. Phys. Commun. **183**, 2458 (2012).

[58] F. Staub, SARAH (2008), arXiv:0806.0538.

[59] Florian Staub, From superpotential to model files for FeynArts and CalcHep/CompHep, Comput. Phys. Commun. **181**, 1077 (2010).

[60] Florian Staub, Automatic calculation of supersymmetric renormalization group equations and self energies, Comput. Phys. Commun. **182**, 808 (2011).

[61] Florian Staub, SARAH 3.2: Dirac gauginos, UFO output, and more, Comput. Phys. Commun. **184**, 1792 (2013).

[62] Florian Staub, SARAH 4: A tool for (not only SUSY) model builders, Comput. Phys. Commun. **185**, 1773 (2014).

[63] Florian Staub, Exploring new models in all detail with SARAH, Adv. High Energy Phys. **2015**, 840780 (2015).

[64] T. Faber, Y. Liu, W. Porod, and J. Jones-Pérez, Revisiting neutrino and sneutrino dark matter in natural SUSY scenarios, Phys. Rev. D **101**, 055029 (2020).

[65] J. Masias, N. Cerna-Velazco, J. Jones-Perez, and W. Porod, Resolving a challenging supersymmetric low-scale seesaw scenario at the ILC, Phys. Rev. D **103**, 115028 (2021).